

Sliding Mode Based Control and Synchronization of Chaotic Systems in Presence of Parametric Uncertainties

Moez Feki

Abstract This chapter deals with the control and synchronization of chaos where both of them are regarded as a case of a control problem. The proposed approach consists in using the sliding mode control theory. We first compare the pioneering OGY control method to the sliding mode control method. We next present a sliding surface design based on the Lyapunov theory. We show that for the class of chaotic systems that can be stabilized using a smooth feedback controller, a sliding manifold can be easily constructed using the Lyapunov function. Besides, we prove that the designed sliding surface is a stable manifold for the originally chaotic system. Thus, should the state behavior be confined to it, then the trajectory will slide towards the equilibrium. We also prove that the proposed controller is robust to mismatched parametric uncertainties. To diminish the effect of the unwanted chattering phenomenon resulting from high sliding gains, an adaptive sliding controller is finally designed to present a robust model independent controller that achieves stabilization of the equilibrium points as well as synchronization of two systems. All these results will be confirmed through numerical simulations on Rossler's system.

Keywords Sliding mode control • Controlling chaos • Parametric uncertainties • Robust control • Adaptive gain • Rossler's system

1 Introduction

Chaotic behavior has been observed in several natural systems such as chaos in the brain [28], cardiac chaos [14], as well as in engineering systems and mainly in power electrical systems [5, 21, 26]. Due to its complexity and unpredictability, designers have more often than not attempted to develop methods to avoid it. During the last three decades, newly developed mathematical and simulation tools incited

M. Feki (✉)

École Supérieure des Sciences et de la Technologie de Hammam Sousse,
University of Sousse, Sousse, Tunisia
e-mail: moez.feki@enig.rnu.tn; wwfekimo@gmail.com

© Springer International Publishing AG 2017

S. Vaidyanathan and C.-H. Lien (eds.), *Applications of Sliding Mode Control in Science and Engineering*, Studies in Computational Intelligence 709,
DOI 10.1007/978-3-319-55598-0_2

researchers to develop methods to harness the very peculiar behavior of chaos. While the first developed methods assume total knowledge of the system to be controlled, recently researchers focused on uncertain chaotic systems. Our present work falls within this new stream, where we present a control method that can achieve control and synchronization of chaotic systems with minimal knowledge of the system.

The interest in controlling chaotic systems has known a boost after the pioneering work of Ott, Grebogi and York (OGY) [25]. Since then several strategies to control chaos have been developed, see [2, 4] and the references therein. A widely considered controlling method consists in adding an input control signal to attempt to stabilize an unstable equilibrium point or an unstable periodic orbit. This input control signal can be constructed using linear state feedback [15, 37] or nonlinear state feedback [32, 37]. PI and PD regulators have also been used for chaos control of Chua's system [18, 38]. Recently, a new method to stabilize the unstable periodic orbit has been developed [24]. This method concerns switched chaotic systems and it is based on perturbation of the switching instances. In most of these cited works, full knowledge of the system model is required.

To circumvent such restrictive requirement, fuzzy controller has been used to control uncertain chaotic systems in [3, 34]. In [35] authors presented an extension of the OGY method to be one based on the sliding mode control concept. In [20, 23, 29] authors used sliding mode controllers to suppress chaos in Lorenz and Liu system with parametric uncertainties. Authors in [12, 30, 31] designed adaptive control laws to stabilize and synchronize a new chaotic system with unknown parameters based on adaptive control theory and Lyapunov stability theory. In [7] we suggested a model independent adaptive controller to efficiently control and synchronize Chua's system with cubic nonlinearity. The synchronization of uncertain chaotic systems has also been considered using robust observer design [8, 10, 13].

In this work we address chaos control using sliding mode theory. First, the OGY method is compared to the sliding mode method where the design of the sliding surface rely on the eigenvectors corresponding to the stable eigenvalues of the system Jacobian. Next, we propose a simple method based on Lyapunov theory to construct the sliding surface. We show that if the states are confined to the sliding surface the originally chaotic system becomes asymptotically stable and the trajectory will slide along the stable manifold until it reaches an equilibrium point. Robustness of the proposed controller with respect to modeling uncertainties is also proven. To decrease the chattering behavior of the sliding control, the sliding gain is adjusted adaptively. We finally confirm our results with numerical simulations on Rossler's system.

This chapter is outlined as follows. In Sect. 2, we present the chaotic Rossler's system and a brief analysis of its behavior. In Sect. 3, we compare the OGY control method to the sliding control strategy. In Sect. 4, we present a sliding surface construction method based on the Lyapunov function, we show the controller design method and we prove its robustness and how to apply it for synchronization. In Sect. 5 we illustrate the efficiency of our method using numerical simulations. Section 6 will be devoted to the adaptive sliding controller design. Finally, conclusions and remarks will be brought in the last section.

2 Rossler's System

In this chapter, we will consider Rossler's system as a workhorse although most of the presented results can be applied to several other well known chaotic systems such as Lorenz system, Chen System or Chua system [11].

The defining equations of the Rossler's system are [27]:

$$\dot{x}_1 = -x_2 - x_3 \quad (1)$$

$$\dot{x}_2 = x_1 + ax_2 \quad (2)$$

$$\dot{x}_3 = b + x_3(x_1 - c) \quad (3)$$

where $x = (x_1, x_2, x_3)^T$ is the state vector and $(a, b, c)^T$ is a parameter vector, here the superscript T denotes the transpose of the vector. Rossler studied the system with $a = 0.2$, $b = 0.2$ and $c = 5.7$. In our simulations, we have used $c = 7$. One of the advantages of Rossler's equations is the linear aspect of the first two equations which can be easily studied on the $x_3 = 0$ plane. Indeed, the second order subsystem

$$\dot{x}_1 = -x_2 \quad (4)$$

$$\dot{x}_2 = x_1 + ax_2 \quad (5)$$

has complex eigenvalues with positive real part for $0 < a < 2$, thus the system trajectory will spiral outwards on the (x_1, x_2) plane. Now, if we consider back the x_3 state, then as far as x_1 is small compared to c , the system behavior keeps close to $x_3 = 0$ plane. Once the system orbit approaches $x_1 \geq c$, the x_3 variable grows exponentially and reverse the dynamics of x_1 that is the states x_1 and x_2 start to decrease.

To make a further analysis, we may easily determine the system fixed points which are:

$$\begin{aligned} x_{eq}^1 &= \left(\frac{c - \sqrt{c^2 - 4ab}}{2}, \frac{-c + \sqrt{c^2 - 4ab}}{2a}, \frac{c - \sqrt{c^2 - 4ab}}{2a} \right) \\ &= (0.5719, -2.8595, 2.8595) \times 10^{-2} \end{aligned} \quad (6)$$

$$\begin{aligned} x_{eq}^2 &= \left(\frac{c + \sqrt{c^2 - 4ab}}{2}, \frac{-c - \sqrt{c^2 - 4ab}}{2a}, \frac{c + \sqrt{c^2 - 4ab}}{2a} \right) \\ &= (6.9943, -34.9714, 34.9714) \end{aligned} \quad (7)$$

We note that the first fixed point is very close to the origin and according to Fig. 1 it resides in the center of the attractor. Whereas the second fixed point does not belong to the attractor and will not be studied in this work.

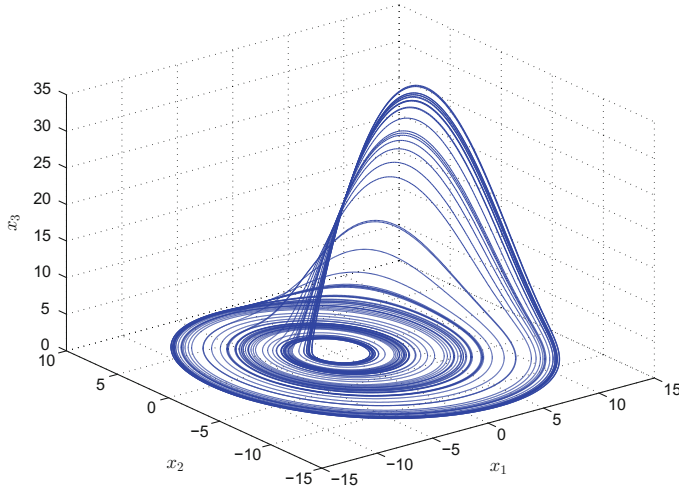


Fig. 1 Rossler's attractor

The behavior of the system in the vicinity of the fixed point can be analyzed through the determination of the eigenvalues and eigenvectors of the Jacobian matrix J .

$$J = \begin{bmatrix} 0 & -1 & -1 \\ 1 & a & 0 \\ x_3^* & 0 & x_1^* - c \end{bmatrix}$$

where x_i^* is the i th component of the fixed point. In our simulations, the eigenvalues are:

$$\lambda_1 = 0.0980 + 0.9951j, \lambda_2 = 0.0980 - 0.9951j, \lambda_3 = -6.9903$$

and the eigenvectors are:

$$V_1 = \begin{pmatrix} 0.7072 \\ -0.0721 - 0.7033j \\ 0.0028 - 0.0004j \end{pmatrix}, V_2 = \begin{pmatrix} 0.7072 \\ -0.0721 + 0.7033j \\ 0.0028 + 0.0004j \end{pmatrix}, V_3 = \begin{pmatrix} 0.1389 \\ -0.0193 \\ 0.9901 \end{pmatrix}$$

Clearly, the plane defined in the state space by V_1 and V_2 is an unstable manifold and the system orbit will be diverging in its direction. However, the line defined in the state space by V_3 is a stable manifold and the system orbit will be converging in its direction.

The overall behavior thus can be described as follows. An orbit within the Rossler attractor starting near the $x_3 = 0$ plane, spirals outwards around the unstable fixed point and close to the plane. As soon as the spiral is large enough, the orbit leaves the $x_3 = 0$ plane in the positive direction while getting closer to the stable manifold.

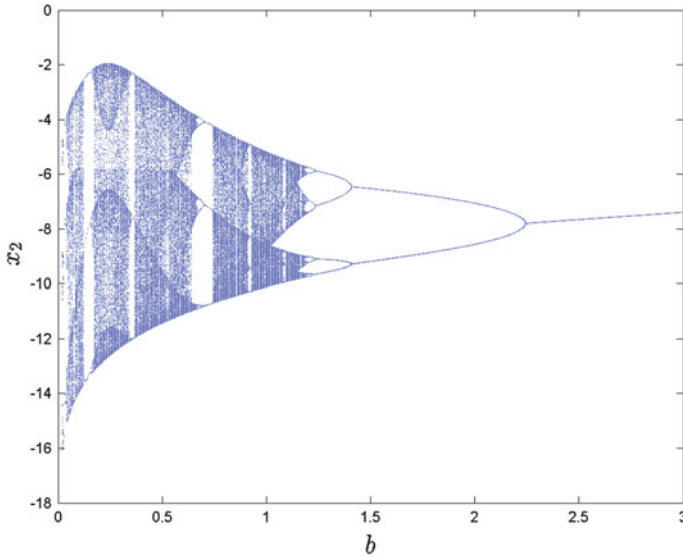


Fig. 2 Bifurcation diagram with varying b

Once the x_1 variable is small enough, the orbit plunges again to the $x_3 = 0$ plane. The behavior is thus dominated by a homoclinic orbit.

In Fig. 2, we show the bifurcation diagram with varying b . It is clear that the system undergoes a series of period doubling bifurcations when the parameter b decreases. We also note the existence of windows of period three behavior within the chaotic region confirming the premise of period three implies chaos [22].

3 The OGY Control Method and Sliding Mode

Consider a continuous time chaotic system defined by:

$$\dot{x} = f(x, p_0), \quad (8)$$

where x is the state vector and p_0 is an accessible parameter vector. We assume that system (8) behaves chaotically for a range of parameter vector p such that $|p - p_0| \leq \Delta p_0$. Let x_0 be an equilibrium point of (8), due to the chaotic nature of the system, x_0 is rather unstable equilibrium and for many well known systems, such as Rossler's system and Chua's system, x_0 is a saddle. Thus, the Jacobian $\frac{\partial f}{\partial x}|_{(x,p)=(x_0,p_0)}$ has stable and unstable eigenvalues respectively denoted λ_s and λ_u . In the case of Rossler system, $\lambda_s = \lambda_3$ and $\lambda_u = (\lambda_1, \lambda_2)$. To these eigenvalues correspond eigenvectors that divide the state space into stable and unstable manifolds \mathcal{M}_s and \mathcal{M}_u . It

is clear that any trajectory $x(t)$ will be moving towards x_0 in the direction of \mathcal{M}_s and getting away from x_0 in the direction of \mathcal{M}_u as it has been already described earlier for Rossler's system.

The OGY control method suggests to use the stable manifold as a vehicle to drive the trajectory $x(t)$ towards the equilibrium x_0 . To achieve this aim, the idea consists in defining a small perturbation $\Delta p(t) < \Delta p_0$ to push the trajectory $x(t)$ onto $\mathcal{M}_s(t)$ (the stable manifold corresponding to the parameter vector $p_0 + \Delta p(t)$). The requirement that $\Delta p(t) < \Delta p_0$ preserves the chaotic property of the system; permitting thereby to use the ergodicity which guarantees that sooner or later $x(t)$ will pass close to \mathcal{M}_s and to use the entropy of the chaotic system to drive its orbit towards x_0 with little efforts.

As a matter of fact, the OGY control method can be interpreted as a special case of the sliding mode control. Indeed, the perturbation of the accessible parameter can be regarded as defining an additional control signal u to push $x(t)$ towards the stable manifold \mathcal{M}_s and keep it thereon for all subsequent times. Once over \mathcal{M}_s , the trajectory $x(t)$ will move towards x_0 . In general, in the sliding mode control theory the additional control u can be any state feedback signal and the sliding surface $\sigma \equiv \mathcal{M}_s$ can be any subspace of the state space that yields to asymptotically stable behavior if the system is confined to it.

In this work, we attempt to stabilize the equilibrium point of Rossler's system x_{eq}^1 . We can easily verify that this equilibrium is saddle type. More precisely, the equilibrium x_{eq}^1 has a stable line and an unstable plane. In \mathbb{R}^3 the line is defined by the intersection of planes that we will denote here σ_1 and σ_2 .

To stabilize the origin, we will consider a perturbation to the parameter b which will be calculated using the sliding mode theory. However, stabilizing x_{eq}^1 using a scalar control signal is not a straight forward task. In fact, to reach our aim, we need to push the trajectory $x(t)$ towards the planes σ_1 and σ_2 simultaneously. To do so, we suggested to push the trajectory $x(t)$ alternately towards the furthest plane; the trajectory $x(t)$ will finally end up on the intersection, that is on the stable line. Eventually, the trajectory $x(t)$ will slide along that line until it reaches x_{eq}^1 . Illustrations of the suggested controller will be presented in Sect. 5.

4 Sliding Mode Controller Design

In this section we present a new method to construct the stable manifold based on the Lyapunov stability theory. In fact, we attempt to avoid the dependence on the eigenvalues and eigenvectors of the Jacobian. The sliding manifold will be kept invariant using a state feedback controller. We show that such construction has several advantages such as robustness to mismatched parametric uncertainties.

4.1 Constructing New Sliding Surface

We consider the following autonomous continuous-time chaotic system:

$$\dot{x} = f(x) , \quad (9)$$

where $x \in \mathbb{R}^n$. An input control signal $u \in \mathbb{R}$ will be applied to stabilize the unstable equilibrium points or to synchronize the system with a master chaotic system. The input signal is injected using a vector field $g(x)$ as follows

$$\dot{x} = f(x) + g(x)u . \quad (10)$$

We suppose that there exists a stabilizing state feedback $\gamma(x)$ such that the closed-loop system

$$\dot{x} = f(x) + g(x) \cdot \gamma(x) , \quad (11)$$

is uniformly asymptotically stable. According to the converse theorem of Lyapunov stability theory [33], there exists a C^∞ Lyapunov function $V(x)$ and class- \mathcal{K} functions $\alpha_i \in \mathcal{K}$ ($i = 1, 2, 3$) such that

- (i) $\alpha_1(\|x\|) \leq V(x) \leq \alpha_2(\|x\|)$
- (ii) $\dot{V}(x) \leq -\alpha_3(\|x\|)$

Now if we choose a nonlinear sliding surface of the form,

$$\sigma(x) = \frac{dV(x)}{dx} g(x) = 0 , \quad (12)$$

then on the sliding surface $\sigma(x) = 0$ the following relations hold for system (11).

$$\dot{V}(x) = \frac{dV(x)}{dx} f(x) + \frac{dV(x)}{dx} g(x) \cdot \gamma(x) \quad (13a)$$

$$\dot{V}(x) = \frac{dV(x)}{dx} f(x) \quad (13b)$$

$$\dot{V}(x) \leq -\alpha_3(\|x\|) \quad (13c)$$

Remark 1 Using equalities (13), we can say that should the system orbit be confined to the specifically chosen sliding surface $\sigma(x) = 0$ defined by (12) the controlled system behaves similarly to the uncontrolled one. In addition, the originally autonomous chaotic system (9) becomes asymptotically stable, and admits $V(x)$ as a Lyapunov function as far as the system trajectory is restricted to $\sigma(x) = 0$.

4.2 Constructing Robust Sliding Controller

In order to restrict the states to the sliding surface we should choose a feedback control that ensures the attractivity of the surface and that guarantees the sliding behavior. To accomplish this aim the necessary condition $\sigma\dot{\sigma} < 0$ should be satisfied. One way, is to choose

$$\dot{\sigma} = -W_1\sigma - W_2\text{sign}(\sigma), \quad W_1 > 0, W_2 > 0, \quad (14)$$

which yields to

$$\sigma\dot{\sigma} = -W_1\sigma^2 - W_2|\sigma| < 0. \quad (15)$$

Knowing that

$$\dot{\sigma} = \frac{d\sigma}{dx}f(x) + \frac{d\sigma}{dx}g(x) \cdot u, \quad (16)$$

and combining with (14) we get

$$u(x) = \frac{-\frac{d\sigma}{dx}f(x) - W_1\sigma(x) - W_2\text{sign}(\sigma(x))}{\frac{d\sigma}{dx}g(x)}. \quad (17)$$

If we apply this feedback control, then the states will be attracted to the surface $\sigma(x) = 0$ and will be confined to it for all subsequent time. The trajectories will then slide along $\sigma(x) = 0$ to the equilibrium point. This inherently means that the equilibrium point should belong to the sliding surface.

From (13) we can deduce that since the effect of the controller vanishes on the sliding surface, then any uncertainties in the system parameters that are used to calculate the feedback law (17) will not affect the behavior of the closed loop system if the states are restricted to the sliding surface.

Fact 1 *The proposed controller (17) is robust to matched and mismatched variations of parameters that are not used to define $\sigma(x) = 0$.*

To prove this fact we consider that the controlled chaotic system is in reality

$$\dot{x} = f(x) + \Delta f(x) + g(x)u, \quad (18)$$

where $f(x)$ is the nominal part of the system and $\Delta f(x)$ represents the uncertainty part. We need to show that the attractivity and sliding condition $\sigma\dot{\sigma} < 0$ is still satisfied.

$$\dot{\sigma} = \frac{d\sigma}{dx}f(x) + \frac{d\sigma}{dx}\Delta f(x) + \frac{d\sigma}{dx}g(x) \cdot u \quad (19)$$

applying (17) yields

$$\dot{\sigma} = -W_1\sigma - W_2\text{sign}(\sigma) + \frac{d\sigma}{dx}\Delta f(x) \quad (20)$$

Let $W_2 > \delta > \left\| \frac{d\sigma}{dx}\Delta f(x) \right\|$

$$\sigma\dot{\sigma} < -W_1\sigma^2 - W_2|\sigma| + \delta|\sigma| \quad (21)$$

$$\sigma\dot{\sigma} < -W_1\sigma^2 - (W_2 - \delta)|\sigma| < 0 \quad (22)$$

Fact 2 *The controller described by*

$$u(x) = \frac{-W_1\sigma(x) - W_2\text{sign}(\sigma(x))}{\frac{d\sigma}{dx}g(x)} . \quad (23)$$

is independent of $f(x)$ and stabilizes the equilibrium points of (9).

The proof of this second fact follows directly from the proof of the first fact by choosing $W_2 > \delta > \left\| \frac{d\sigma}{dx}f(x) \right\|$.

4.3 Synchronization Using Sliding Mode Controller

The chaotic synchronization problem can be regarded as an output tracking problem [6]. We consider the slave system (10) with the following output

$$y = h(x) , \quad (24)$$

We suppose that if the output y becomes equal to the output y_m of a master chaotic system then states of the master and slave system will be synchronized. This hypothesis is not restrictive as it can be satisfied by many chaotic systems in literature, such as Rossler and Lorenz system [9] Chua's system [7], and jerk systems [6] with $h(x) = x_1$.

Thus, to obtain synchronization, we want $y(t)$ to be equal to $y_m(t)$. Now let's assume that system (10) with the output (24) has relative degree $\rho = n$ (see [16]). Therefore we can define a nonlinear transformation $z = \phi(x)$

$$z_1 = h(x) , \quad z_{i+1} = L_f^i h(x) , \quad i = 1, \dots, n-1 .$$

Using z as the new state variable, system (10) becomes

$$\dot{z}_i = z_{i+1} , \quad i = 1, \dots, n-1 , \quad (25a)$$

$$\dot{z}_n = F(z) + G(z)u , \quad (25b)$$

with $y = z_1$, $F(z) = L_f^n h(\Phi^{-1}(z))$ and $G(z) = L_g L_f^{n-1} h(\Phi^{-1}(z))$. We want to design a feedback control that forces the output y to track y_m . To accomplish this aim we define a tracking error $e = Y_m - z$ where $Y_m = (y_m, \dot{y}_m, \dots, y_m^{(n-1)})^T$. The error dynamics are described by

$$\dot{e}_i = e_{i+1}, \quad i = 1, \dots, n-1, \quad (26a)$$

$$\dot{e}_n = y_m^{(n)} - F(Y_m - e) - G(Y_m - e)u. \quad (26b)$$

It is well known that the smooth controller

$$\gamma(e) = \frac{1}{G(z)} (-F(z) + y_m^{(n)} + K^T e), \quad (27)$$

with $K = (k_1, k_2, \dots, k_n)^T$, leads to a linear closed loop system that can be written as $\dot{e} = Ae$

$$\begin{bmatrix} \dot{e}_1 \\ \dot{e}_2 \\ \vdots \\ \dot{e}_{n-1} \\ \dot{e}_n \end{bmatrix} = \begin{bmatrix} 0 & 1 & 0 & \dots & 0 \\ 0 & 0 & 1 & \dots & 0 \\ \vdots & \vdots & \ddots & \ddots & \vdots \\ \vdots & \vdots & \vdots & \ddots & 1 \\ -k_1 & -k_2 & -k_3 & \dots & -k_n \end{bmatrix} \begin{bmatrix} e_1 \\ e_2 \\ \vdots \\ e_{n-1} \\ e_n \end{bmatrix}. \quad (28)$$

Eventually, the problem is solved if K is chosen such that all the roots of the polynomial

$$p(s) = s^n + k_n s^{n-1} + \dots + k_3 s^2 + k_2 s + k_1$$

have negative real parts. Indeed we have

$$\lim_{t \rightarrow \infty} e(t) = 0 \Leftrightarrow \lim_{t \rightarrow \infty} z(t) = Y_m,$$

Taking the inverse transformation $x = \phi^{-1}(z)$ and $x_m = \phi^{-1}(Y_m)$, we easily deduce that synchronization is achieved, i.e.

$$\lim_{t \rightarrow \infty} x(t) = x_m(t).$$

We now have shown that a smooth stabilizing control law exists for the error dynamic system. Since (28) is a linear system, it is easy to find a Lyapunov function $V(e)$ in the form $V(e) = e^T P e$ where $P > 0$ is a positive definite matrix such that $\dot{V}(e) = -e^T Q e$, $Q > 0$. Next we construct a sliding surface

$$\sigma_e = -\frac{dV(e)}{de_n} G(Y_m - e) = 0.$$

Hence using (17) we obtain an expression for the feedback sliding control law

$$u(e) = \frac{-\frac{d\sigma_e}{de}F(e) - W_1\sigma_e - W_2\text{sign}(\sigma_e)}{\frac{d\sigma_e}{de}G(e)}. \quad (29)$$

where

$$F(e) = \begin{pmatrix} e_2 \\ \vdots \\ e_n \\ y_m^{(n)} - F(Y_m - e) \end{pmatrix}, \quad G(e) = \begin{pmatrix} 0 \\ \vdots \\ 0 \\ -G(Y_m - e) \end{pmatrix}$$

$u(e)$ will force trajectories of (26) to slide on the surface σ_e until they reach $e = 0$ and consequently synchronization will be achieved.

5 Illustrative Example

The controlled Rossler system that we will consider in this section is merely similar to the one presented in Sect. 2 with a control signal u added to the dynamics of x_3 :

$$\dot{x}_1 = -x_2 - x_3 \quad (30a)$$

$$\dot{x}_2 = x_1 + ax_2 \quad (30b)$$

$$\dot{x}_3 = b + x_3(x_1 - c) + u \quad (30c)$$

System (30) is in the form of (10) and the addition of signal u makes $g(x) = (0, 0, 1)^T$ besides it can be regarded as a perturbation to the parameter b .

5.1 Sliding Mode Control Issued from the OGY Method

Eigenvectors corresponding to x_{eq}^1 have been calculated in Sect. 2 and V_3 defines the stable manifold \mathcal{M}_s which is a line passing through x_{eq}^1 . To define σ_1 and σ_2 , we just need to choose two vectors V_{31} and V_{32} that may or not be orthogonal to V_3 and to each other. In fact, they just need to be linearly independent. Then V_{31} and V_{32} will be considered as the normals to σ_1 and σ_2 respectively. Therefore we have:

$$\sigma_1(x) = V_{31}^T(x - x_{eq}^1) \quad (31)$$

$$\sigma_2(x) = V_{32}^T(x - x_{eq}^1) \quad (32)$$

and

$$\frac{\sigma_1(x)}{dx}f(x) = V_{31}^T f(x) \qquad \frac{\sigma_2(x)}{dx}f(x) = V_{32}^T f(x) \quad (33)$$

$$\frac{\sigma_1(x)}{dx}g(x) = V_{31}(3) \qquad \frac{\sigma_2(x)}{dx}g(x) = V_{32}(3) \quad (34)$$

where $V(i)$ is the i th component of vector V . It follows that from the expression of the controller $u(x)$ 17, we need to have a non zero third components in V_{31} and V_{32} . Next, we present two choices for V_{31} and V_{32} .

5.1.1 Choice Leading to First Order Sliding Mode

In this case, we have chosen:

$$V_{31} = \left(\frac{1}{V_3(1)}, -\frac{1}{2V_3(2)}, -\frac{1}{2V_3(3)} \right)^T \quad (35)$$

and

$$V_{32} = \left(\frac{\frac{1}{2V_3(2)} - \frac{V_3(2)}{2V_3(3)^2}}{\frac{1}{V_3(1)} + \frac{V_3(1)}{2V_3(3)^2}}, 1, -\frac{V_3(1)}{V_3(3)} \frac{\frac{1}{2V_3(2)} - \frac{V_3(2)}{2V_3(3)^2}}{\frac{1}{V_3(1)} + \frac{V_3(1)}{2V_3(3)^2}} - \frac{V_3(2)}{V_3(3)} \right)^T \quad (36)$$

We can easily verify that V_3 , V_{31} and V_{32} are orthogonal to each other thus to surfaces σ_1 and σ_2 will also be orthogonal. Applying the control signal $u(x)$ 17 such that the system orbit will be attracted to the furthest surface leads to the results presented in Figs. 3 and 4. First, we need to mention here that we have saturated the controller at $U_{\max} = 10$ to avoid large controller values in transients. We have also used $W_1 = 0$ and $W_2 = 5$ as controller gains and the controller has been switched on at time $t = 100$ s.

Clearly, the stabilization has been achieved although the controller signal amplitude is quite large that it cannot be really considered simply as a parameter perturbation. Besides, the chattering phenomenon is dominating the controller signal once the equilibrium is reached.

5.1.2 Choice Leading to Second Order Sliding Mode

In this case, we have chosen:

$$V_{31} = \left(-\frac{1}{V_3(1)}, \frac{1}{V_3(2)}, 0 \right)^T \quad (37)$$

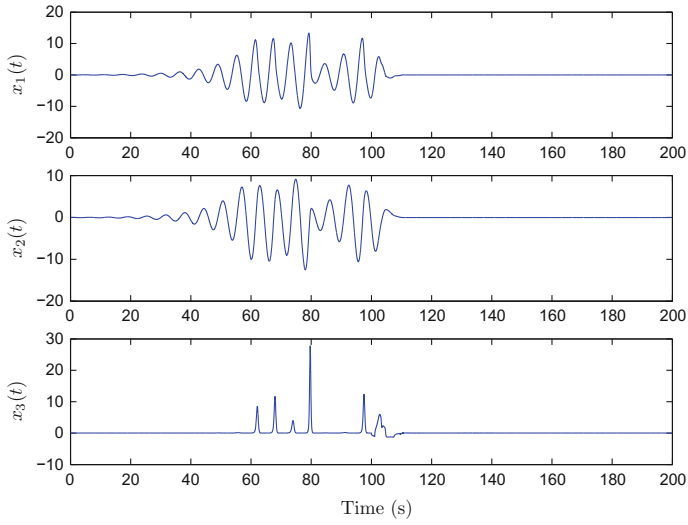


Fig. 3 Stabilization of x_{eq}^1 using first order sliding mode issued from OGY idea

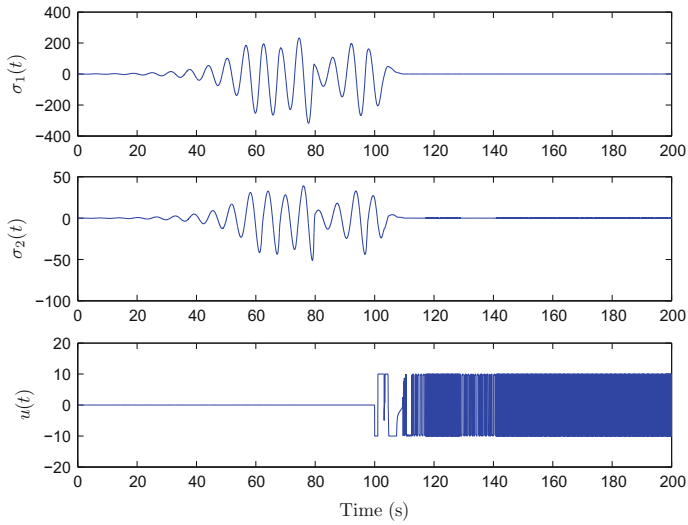


Fig. 4 Time evolution of σ_1 and σ_2 and the sliding mode controller

and

$$V_{32} = \left(\frac{1}{V_3(2)}, \frac{1}{V_3(1)}, -\frac{V_3(1)^2 + V_3(2)^2}{V_3(1)V_3(2)V_3(3)} \right)^T \quad (38)$$

With this choice 16 will not immediately lead to the expression of $u(x)$ when using σ_1 since

$$\dot{\sigma}_1 = \frac{d\sigma_1}{dx}f(x) + \frac{d\sigma_1}{dx}g(x) \cdot u = \frac{d\sigma_1}{dx}f(x) \quad (39)$$

therefore, to obtain $u(x)$, we need to determine the second time derivative of $\sigma_1(x)$ and thus to reach sliding mode we will need to have $\sigma_1(x) = 0$ and $\dot{\sigma}_1(x) = 0$ which means that we will reach a second order sliding mode. One of the main advantages of this fact is the decrease or the annihilation of the chattering phenomenon [1, 17, 36].

$$\begin{aligned} \ddot{\sigma}_1 &= V_{31}(1)(-\dot{x}_2 - \dot{x}_3) + V_{31}(2)(\dot{x}_1 + a\dot{x}_2) \\ &= V_{31}(1)(-x_1 - ax_2 - b - x_3(x_1 - c)) + V_{31}(2)(-x_2 - x_3 + a(x_1 + ax_2)) \\ &\quad - V_{31}(1)u \\ &= \mathcal{A}(x) + \mathcal{B}(x)u \end{aligned}$$

by applying

$$u(x) = \frac{-\mathcal{A}(x) - W_{11}\sigma_1(x) - W_{21}\text{sign}(\sigma_1(x)) - W_{12}\dot{\sigma}_1(x) - W_{22}\text{sign}(\dot{\sigma}_1(x))}{\mathcal{B}(x)} \quad (40)$$

to make σ_1 attractive and applying

$$u(x) = \frac{-\frac{d\sigma_2}{dx}f(x) - W_1\sigma_2(x) - W_2\text{sign}(\sigma_2(x))}{\frac{d\sigma_2}{dx}g(x)} . \quad (41)$$

to make σ_2 attractive, we achieve intermitting between first and second order sliding mode. The results obtained in this case are depicted in Figs. 5 and 6. In this case, we have saturated the controller at $U_{\max} = 15$ to avoid large controller values in transients. We have also used the following controller gains

$$W_1 = 0.1, W_{11} = 0.01, W_{12} = 0.2$$

$$W_2 = 40, W_{21} = 40, W_{22} = 40$$

again the controller has been switched on at time $t = 100$ s. On Fig. 6, we clearly notice the discontinuities in the controller signal at the transient time due to the switchings from one controller to another. In addition, we notice the absence of the chattering phenomenon due to the second order sliding mode.

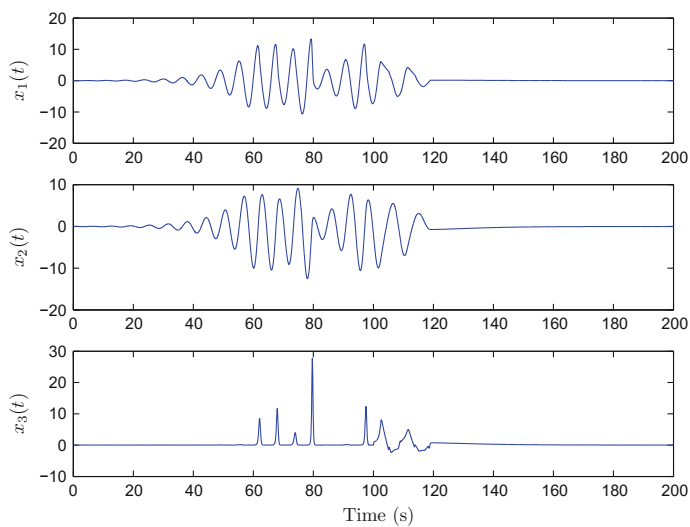


Fig. 5 Stabilization of x_{eq}^1 using second order sliding mode issued from OGY idea

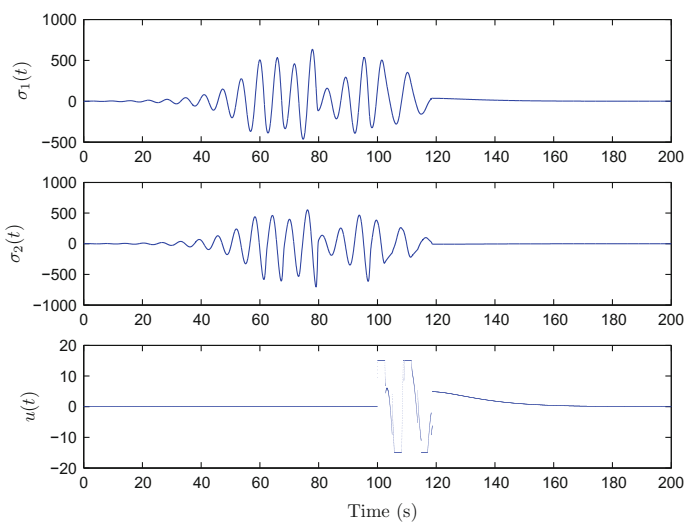


Fig. 6 Time evolution of σ_1 and σ_2 and the sliding mode controller

5.2 New Sliding Mode Control

If we choose $h(x) = x_2$ then we can define the state transformation $\Phi(x)$ as follows:

$$\Phi(x) = \begin{bmatrix} z_1 \\ z_2 \\ z_3 \end{bmatrix} = \begin{bmatrix} x_2 \\ x_1 + ax_2 \\ ax_1 + (a^2 - 1)x_2 - x_3 \end{bmatrix}.$$

Using z as state variable, system (30) becomes:

$$\dot{z}_1 = z_2, \quad (42a)$$

$$\dot{z}_2 = z_3, \quad (42b)$$

$$\dot{z}_3 = F(z) + G(z)u. \quad (42c)$$

where $G(z) = -1$. We now follow the design steps described in Sect. 4. We let $K = (8, 12, 6)^T$ and choose the Lyapunov function $V(e) = e^T P e$ with

$$P = \frac{1}{512} \begin{bmatrix} 4880 & 3160 & 160 \\ 3160 & 5360 & 370 \\ 160 & 370 & 275 \end{bmatrix}$$

so that $\dot{V}(e) = -5\|e\|^2$. Therefore, the sliding surface becomes:

$$\sigma_e = \frac{1}{256}(160e_1 + 370e_2 + 275e_3) = 0$$

Finally the construction of the sliding mode controller (29) is straight forward. It is worth noting that $\sigma(e)$ and $\frac{d\sigma_e}{de} \mathcal{G}(e)$ do not depend on system parameters.

Figures 7 and 8 show, the stabilization of the equilibrium point x_{eq}^1 which is regarded as tracking a time-invariant trajectory. For the numerical simulations, we used an initial condition $x_{ini} = (7, 2, 0)$ and a sliding gain $W_2 = 4$ whereas $W_1 = 2$. The sliding mode controller is applied at time $t = 100$ s. We clearly see that when $\sigma_e = 0$, sliding starts with a chattering phenomenon.

To investigate the robustness of the suggested controller as explained by Fact 1, we consider that the system parameters are perturbed by 10%. Figures 9 and 10 delineate the stabilization of the equilibrium point and therefore the robustness of the controller to mismatched perturbation.

Figure 11 shows that the trajectories diverge from each other due to sensitivity to the initial condition ($x_{ini}^m = (7, 2, 0.1)$ and $x_{ini}^s = (7, 2, 0)$) and due to mismatched parameters. However, as soon as the controller is applied synchronization is achieved.

In the design of the sliding mode controller (29), the main encountered difficulty is to construct the nonlinear part $\frac{d\sigma_e}{de} \mathcal{F}(e)$, due to the nonlinear expressions it could contain and the need for the system parameters. Actually, we have shown that the

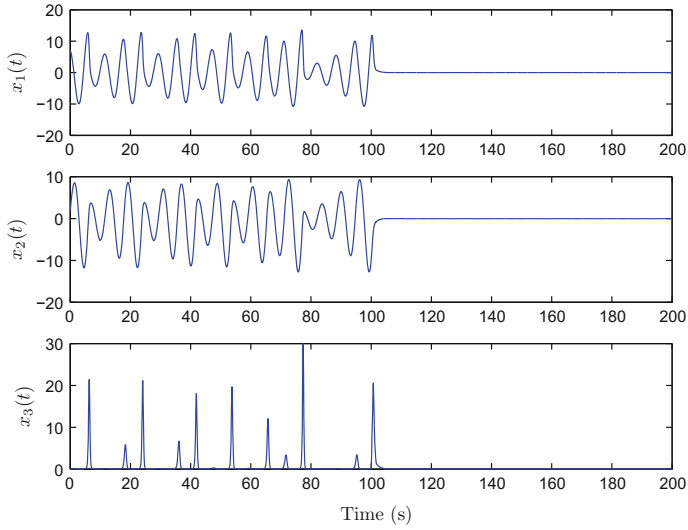


Fig. 7 Stabilization of the unstable equilibrium point x_{eq}^1

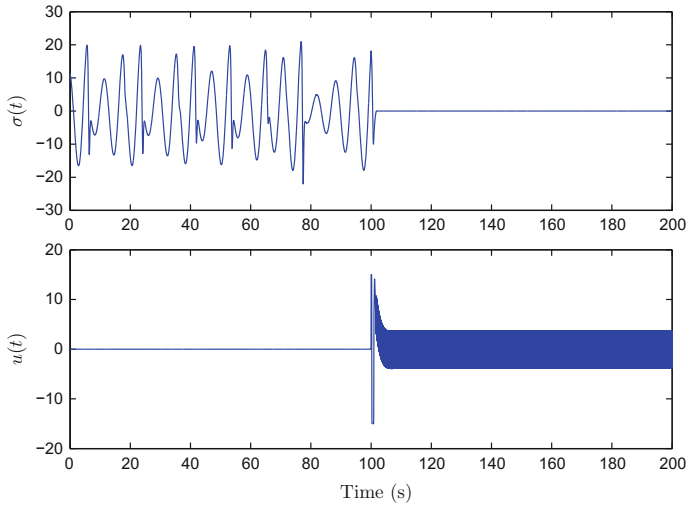


Fig. 8 Time evolution of the switching function and the sliding mode controller

controller is robust to parameters variation. Furthermore, should we choose the sliding gain W_2 such that $\|\frac{d\sigma_e}{de}\mathcal{F}(e)\| < W_2$, then we can use the following sliding controller (as explained by Fact 2):

$$u(e) = \frac{-W_1\sigma_e - W_2\text{sign}(\sigma_e)}{\frac{d\sigma_e}{de}\mathcal{G}(e)}. \quad (43)$$

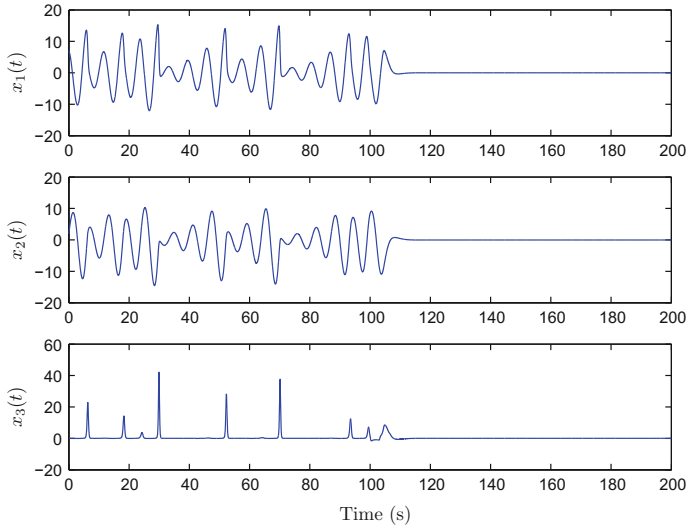


Fig. 9 Stabilization of the unstable equilibrium point x_{eq}^1 in presence of 10% perturbation

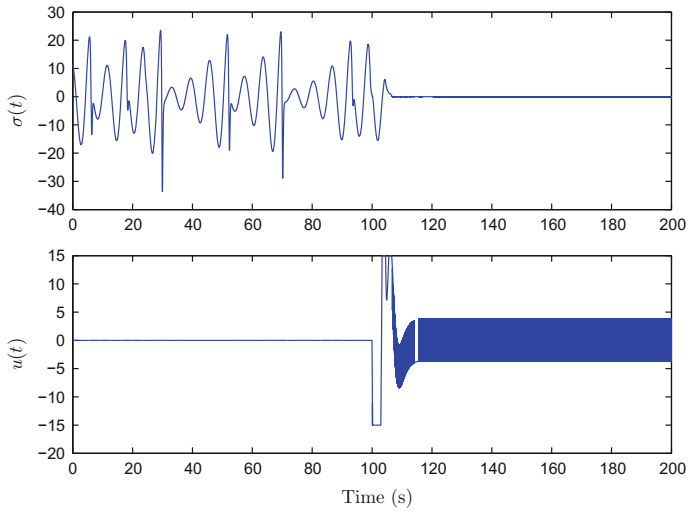


Fig. 10 Time evolution of the switching function and the sliding mode controller in presence of 10% perturbation

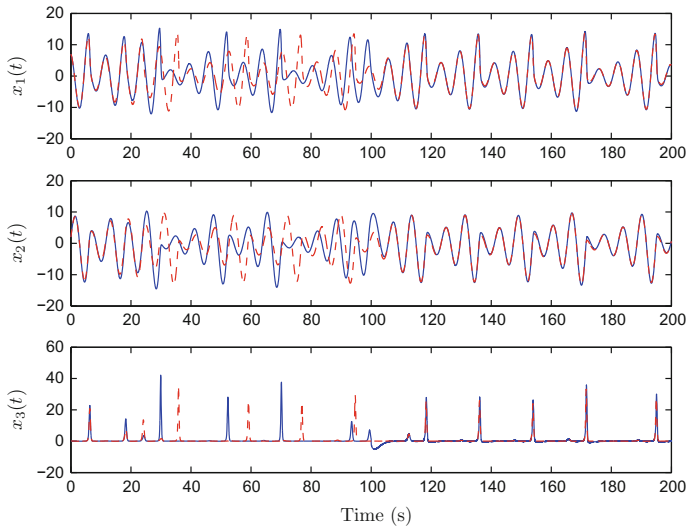


Fig. 11 Synchronization of two Rossler's systems, ($W_2 = 50$ and $W_1 = 10$)

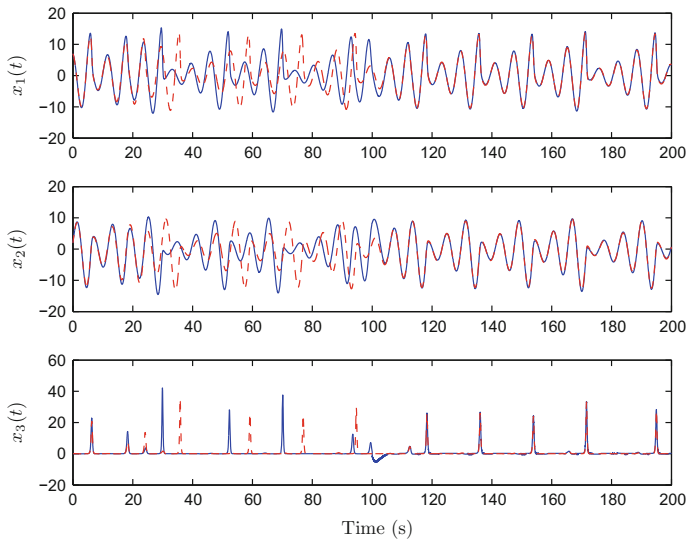


Fig. 12 Synchronization of two Rossler's systems in presence of 10% perturbation, ($W_2 = 150$ and $W_1 = 0$)

Figure 12 depicts the evolution of the state variables and Fig. 13 depicts the sliding controller used to synchronize two Rossler's systems using the robust controller (43) with $W_2 = 150$ and $W_1 = 0$.

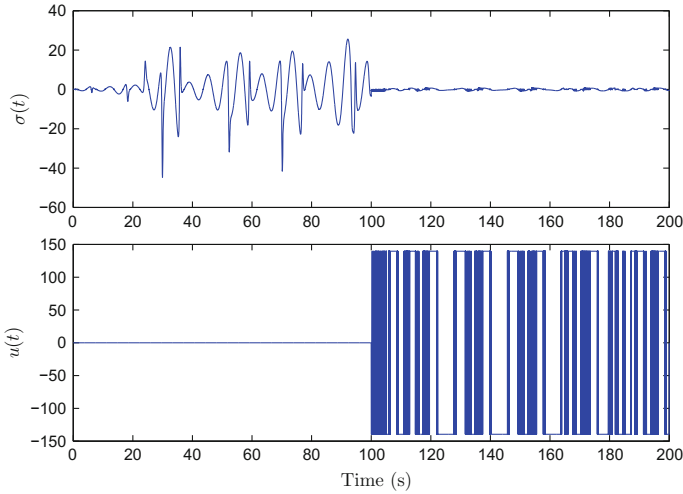


Fig. 13 Time evolution of the switching function and the sliding mode controller with model independent expression

6 Adaptive Sliding Controller Design

The controller suggested in (43) though efficient to synchronize two Rossler's systems, it has two drawbacks: The estimation of an upper boundary of $\|\frac{d\sigma_e}{de}F(e)\|$ is not a simple task, besides, fixing W_2 at a high level yields to unwanted high chattering phenomenon which was indeed at about 150 which is a large control signal due to the fact that it needs to control a large signal $x_3 \approx 30$ with relatively fast dynamics.

To circumvent the aforementioned drawbacks, we suggest to substitute an adapted sliding gain $W_2(t)$ for the fixed one such that

$$W_2(t) > \left\| \frac{d\sigma_e}{de} F(e) \right\|. \quad (44)$$

We will tackle our problem by considering the system

$$\dot{\sigma}_e = \frac{d\sigma_e}{de} F(e) + \frac{d\sigma_e}{de} G(e)u \quad (45)$$

and design the signal u such that $\sigma_e = 0$ is attained. This can be obtained by applying an adaptive linear controller

$$u_{ad}(\sigma_e) = \tilde{\kappa}(t)\sigma_e(t). \quad (46)$$

The adaptive linear controller is guaranteed to yield $\sigma_e = 0$ if it mimics the following linearizing controller [6]

$$u_{lin}(\sigma_e) = \frac{-\frac{d\sigma_e}{de}\mathcal{F}(e) - \kappa\sigma_e}{\frac{d\sigma_e}{de}\mathcal{G}(e)} \quad \kappa > 0. \quad (47)$$

That is in the limit we have

$$u_{ad}^*(\sigma_e) = \tilde{\kappa}^*(t)\sigma_e(t) = u_{lin}(\sigma_e)$$

where $\tilde{\kappa}^*(t)$ is the constant limit of $\tilde{\kappa}(t)$

Fact 3 The adaptive linear controller described in (46) where

$$\tilde{\kappa}(t) = -\int_0^t \left(\gamma \frac{d\sigma_e}{de} \mathcal{G}(e) \sigma_e^2 \right) dt, \quad \gamma > 0 \quad (48)$$

yields to $\sigma_e = 0$.

To prove this fact, we proceed as follows:

$$\begin{aligned} \dot{\sigma}_e &= \frac{d\sigma_e}{de}\mathcal{F}(e) + \frac{d\sigma_e}{de}\mathcal{G}(e)u_{ad} \\ &= \frac{d\sigma_e}{de}\mathcal{F}(e) + \frac{d\sigma_e}{de}\mathcal{G}(e)u_{lin} - \frac{d\sigma_e}{de}\mathcal{G}(e)(u_{lin} - u_{ad}) \\ &= -\kappa\sigma_e - \frac{d\sigma_e}{de}\mathcal{G}(e)(u_{lin} - u_{ad}) \\ &= -\kappa\sigma_e - \frac{d\sigma_e}{de}\mathcal{G}(e)(\tilde{\kappa}^*(t) - \tilde{\kappa}(t))\sigma_e \end{aligned}$$

Now we consider a Lyapunov function candidate

$$V(\sigma_e, \tilde{\kappa}) = \frac{1}{2}\sigma_e^2 + \frac{1}{2\gamma}(\tilde{\kappa}^* - \tilde{\kappa})^2$$

$$\begin{aligned} \dot{V}(\sigma_e, \tilde{\kappa}) &= \sigma_e \dot{\sigma}_e - \frac{1}{\gamma}(\tilde{\kappa}^* - \tilde{\kappa})\dot{\tilde{\kappa}} \\ &= -\kappa\sigma_e^2 - (\tilde{\kappa}^* - \tilde{\kappa})\left(\frac{d\sigma_e}{de}\mathcal{G}(e)\sigma_e^2 + \frac{1}{\gamma}\dot{\tilde{\kappa}}\right) \end{aligned}$$

Therefore, if we choose $\tilde{\kappa}$ as in (48), the time derivative of the Lyapunov function becomes

$$\dot{V}(\sigma_e, \tilde{\kappa}) = -\kappa\sigma_e^2 < 0, \quad \forall \sigma_e \neq 0$$

We can deduce that

$$\dot{\sigma}_e = -\kappa \sigma_e - \frac{d\sigma_e}{de} \mathcal{G}(e) (\tilde{\kappa}^*(t) - \tilde{\kappa}(t)) \sigma_e \quad (49)$$

is stable and hence $\sigma_e \in L_\infty$. Moreover, we have

$$\int_0^t \sigma_e^2 dt = \frac{V(0) - V(t)}{\kappa}.$$

Since $V(t) \in L_\infty$ and $V(0)$ is finite, this implies that $\sigma_e \in L_2$. Also from (49) we obviously have $\dot{\sigma}_e \in L_\infty$ in addition to $\sigma_e \in L_\infty$ and $\sigma_e \in L_2$. Eventually by Barbalat's lemma [19] $\lim_{t \rightarrow \infty} \sigma_e(t) = 0$. This ends the proof of Fact 3.

Now since by construction of u_{ad} , when $\tilde{\kappa}(t)$ reaches its limit we have

$$\tilde{\kappa}(t) \sigma_e(t) = u_{lin}(\sigma_e)$$

then using (46) and (47) we get

$$\frac{d\sigma_e}{de} \mathcal{F}(e) = - \left(\frac{d\sigma_e}{de} \mathcal{G}(e) \tilde{\kappa}(t) + \kappa \right) \sigma_e \quad (50)$$

Finally, to satisfy the sliding condition we need to choose the adaptive sliding gain as follows

$$W_2(t) = \left| \frac{d\sigma_e}{de} \mathcal{G}(e) \tilde{\kappa}(t) + \kappa \right| \cdot |\sigma_e| + \eta, \quad \eta > 0. \quad (51)$$

Eventually, the adaptive sliding controller is given by the following expression

$$u(e) = \frac{-W_1 \sigma_e - W_2(t) \text{sign}(\sigma_e)}{\frac{d\sigma_e}{de} \mathcal{G}(e)}. \quad (52)$$

where $W_2(t)$ is given in (51). We can verify that this controller does not depend on the system parameter since the controller was injected with a constant function $g(x) = (0, 0, 1)^T$.

Figures 14 and 15 depict the obtained results when applying the adaptive sliding controller on Rossler's system. The design parameters are

$$\kappa = 1, \quad \eta = 10, \quad \gamma = 5 \times 10^{-8}$$

Figure 14 shows that synchronization is achieved with an adaptive sliding controller that does not induce high chattering phenomenon. Figure 15 depicts the evolution of the sliding function and of the sliding gain $W_2(t)$. We notice that this gain is large when the controller action starts, as soon as the synchronization is attained, the

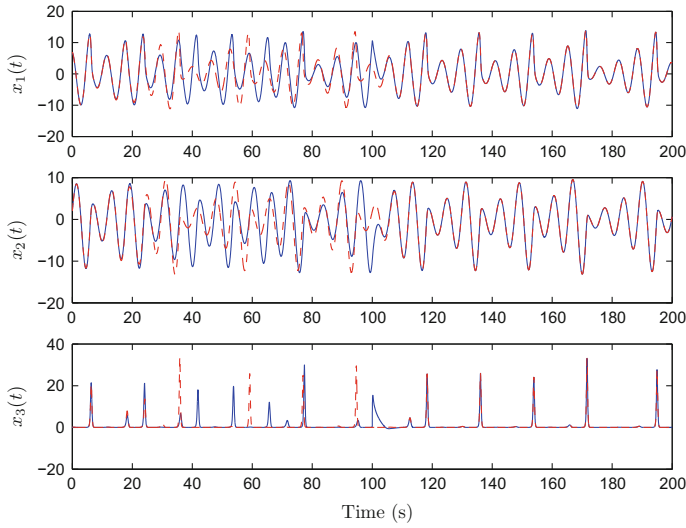


Fig. 14 Synchronization of two Rossler's systems using sliding mode controller with adaptive gain $W_2(t)$

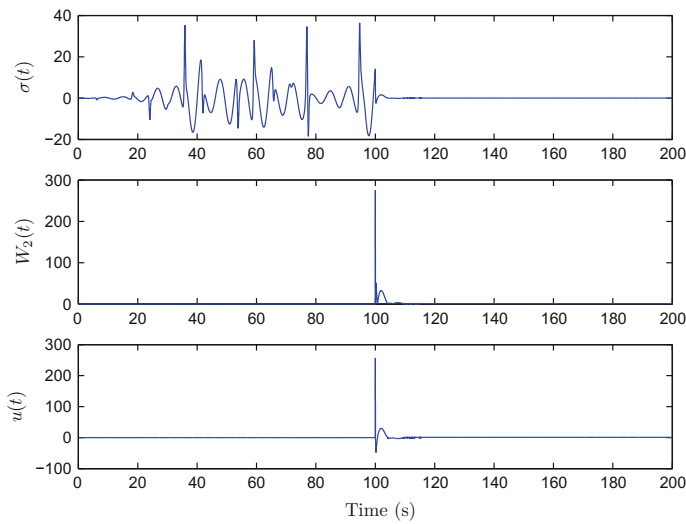


Fig. 15 Time evolution of the switching function, the adaptive sliding gain $W_2(t)$ and the adaptive sliding mode controller with model independent expression

value of $W_2(t)$ decreases and it is less than 40 at $t = 102$ s and less than 5 at $t = 105$ s which is relatively low compared to $W_2 = 150$ set for a non-adaptive robust controller. Therefore, a low chattering phenomenon is obtained.

7 Conclusion

In this work, we have proposed a sliding controller that can be used for chaos control as well as for synchronization of chaotic systems. The sliding surface design is based on a Lyapunov function. The main advantage of this choice is that when confined to the sliding surface the behavior of the controlled system becomes similar to the uncontrolled system. In addition, with this particular choice, we have shown that the sliding controller is robust to mismatched perturbation.

As an improvement of the proposed method we have thought of simplifying the design procedure of the controller meanwhile decreasing its dependence to system parameters and model. Indeed, the obtained adaptive sliding mode controller achieves synchronization of two Rossler's systems with low chattering phenomenon and without implementing complex nonlinear functions.

References

1. Behjameh MR, Delavari H, Vali A (2015) Global finite time synchronization of two nonlinear chaotic gyros using high order sliding mode control. *J Appl Comput Mech* 01(01):26–34
2. Boccaletti S, Grebogi C, Lai YC, Mancini H, Maza D (2000) The control of chaos: theory and applications. *Phys Rep* 329:103–197
3. Chang W, Park J, Joo Y, Chen G (2003) Static output-feedback fuzzy controller for chen's chaotic system with uncertainties. *Inf Sci* 151:227–244
4. Chen G (1999) Controlling chaos and bifurcations in engineering systems. CRC-Press
5. Di Bernardo M, Tse C (2002) Chaos in power electronics: an overview. In: Chen G, Ueta T (eds) *Chaos in circuits and systems*, chap. 16, vol 11. World Scientific, New York, pp 317–340
6. Feki M (2003) An adaptive feedback control of linearizable chaotic systems. *Chaos Solitons Fractals* 15:883–890
7. Feki M (2004) Model-independent adaptive control of chua's system with cubic nonlinearity. *Int J Bifurc Chaos* 14(12):4249–4263
8. Feki M (2004) Synchronization of chaotic systems with parametric uncertainties using sliding observers. *Int J Bifurc Chaos* 14(7):2467–2475
9. Feki M (2006) Synchronization of generalized lorenz system using adaptive controller. In: *IFAC conference on analysis and control of chaotic systems CHAOS'06*, CD-ROM. Reims-France (2006)
10. Feki M (2009) Observer-based synchronization of chaotic systems with unknown nonlinear function. *Chaos Solitons Fractals* 39:981–990
11. Feki M (2009) Sliding mode control and synchronization of chaotic systems with parametric uncertainties. *Chaos Solitons Fractals* 41:1390–1400
12. Fourati A, Feki M, Derbel N (2010) Stabilizing the unstable periodic orbits of a chaotic system using model independent adaptive time-delayed controller. *Nonlinear Dyn* 62(3):687–704
13. Gammoudi IE, Feki M (2013) Synchronization of integer order and fractional order chua's systems using robust observer. *Commun Nonlinear Sci Numer Simul* 18(3):625–638
14. Garfinkel A, Spano ML, Ditto WL, Weiss JN (1992) Controlling cardiac chaos. *Science* 257:1230–1235
15. Hwang CC, Hsieh JY, Lin RS (1997) A linear continuous feedback control of chua's circuit. *Chaos Solitons Fractals* 8:1507–1515
16. Isidori A (1995) *Nonlinear control systems*, 3rd edn. Springer, United Kingdom

17. Jemaâ-Boujelben SB, Feki M (2016) Integral higher order sliding mode control for mimo uncertain systems: application to chaotic prmsm. In: Proceedings of engineering & technology (PET), pp. 632–637. Hammamet-Tunisia
18. Jiang GP, Chen G, Tang WKS (2002) Stabilizing unstable equilibrium points of a class of chaotic systems using a state pi regulator. *IEEE Trans Circuits Syst I* 49(12):1820–1826
19. Khalil HK (1992) *Nonlinear systems*. Macmillan, New York
20. Konishi K, Hirai M, Kokame H (1998) Sliding mode control for a class of chaotic systems. *Phys Lett A* 245:511–517
21. Koubaâ K, Feki M (2014) Quasi-periodicity, chaos and coexistence in the time delay controlled two-cell dc-dc buck converter. *Int J Bifurc Chaos* 24(10): 1450124
22. Li TY, Yorke JA (1975) Period three implies chaos. *Am Math Mon* 82(10):985–992
23. Lin JS, Yan JJ, Liao TL (2006) Robust control of chaos in lorenz systems subject to mismatch uncertainties. *Chaos Solitons Fractals* 27:501–510
24. Miladi Y, Feki M, Derbel N (2015) Stabilizing the unstable periodic orbits of a hybrid chaotic system using optimal control. *Commun Nonlinear Sci Numer Simul* 20:1043–1056
25. Ott E, Grebogi C, Yorke JA (1990) Controlling chaos. *Phys Rev Lett* 64:1196–1199
26. Robert B, Feki M, Iu H (2006) Control of a pwm inverter using proportional plus extended time-delayed feedback. *Int J Bifurc Chaos* 16(1):113–128
27. Rössler O (1976) An equation for continuous chaos. *Phys Lett A* 57(5):397–398
28. Schiff S, Jerger K, Duong D, Chang T, Spano M, Ditto W (1994) Controlling chaos in the brain. *Nature* 370:615–620
29. Sundarapandian V (2012) Global chaos control of hyperchaotic liu system via sliding control method. *Int J Control Theory Appl* 5(2):117–123
30. Sundarapandian V (2013) Analysis and adaptive synchronization of two novel chaotic systems with hyperbolic sinusoidal and cosinusoidal nonlinearity and unknown parameters. *J Eng Sci Technol Rev* 6(4):53–65
31. Sundarapandian V, Pehlivan I (2012) Analysis, control, synchronization, and circuit design of a novel chaotic system. *Math Comput Model* 55(7–8):1904–1915
32. Tian YC, Tade MO, Levy D (2002) Constrained control of chaos. *Phys Lett A* 296:87–90
33. Vidyasagar M (1993) *Nonlinear systems analysis*, 2nd edn. Prentice Hall, New Jersey
34. Yang CH, Wu CL, Chen YJ, Shiao SH (2015) Reduced fuzzy controllers for lorenz-stenflo system control and synchronization. *Int J Fuzzy Syst* 17(2):158–169
35. Yu X, Chen G, Xia Y, Song Y, Cao Z (2001) An invariant-manifold-based method for chaos control. *IEEE Trans Circuits Syst I* 48(8):930–937
36. Zhan-Shan Z, Jing Z, Gang D, Da-Kun Z (2015) Chaos synchronization of coronary artery system based on higher order sliding mode adaptive control. *Acta Phys Sin* 64(21): 210–508
37. Zhang H, Ma X-K, Li M, Zou J-L (2005) Controlling and tracking hyperchaotic rössler system via active backstepping design. *Chaos Solitons Fractals* 26: 353–361
38. Zou YL, Luo XS, Jiang P-Q, Wang BH, Chen G, Fang JQ, Quan HJ (2003) Controlling the chaotic n -scroll chua's circuit. *Int J Bifurc Chaos* 13(9): 2709–2714

Applications of Sliding Mode Control in Science and
Engineering

Vaidyanathan, S.; Lien, C.-H. (Eds.)

2017, XI, 470 p. 246 illus., 236 illus. in color., Hardcover

ISBN: 978-3-319-55597-3